Suppression of Nonlinear Interactions in Resonant Macroscopic Quantum Devices: The Example of the Solid-State Ring Laser Gyroscope

Sylvain Schwartz,[1,*] François Gutty,[2] Gilles Feugnet,[1] Philippe Bouyer,[3] and Jean-Paul Pocholle[1]

[1]*Thales Research and Technology France, RD 128, F-91767 Palaiseau Cedex, France*
[2]*Thales Avionics, 40 rue de la Brelandière, BP 128, F-86101 Châtellerault, France*
[3]*Laboratoire Charles Fabry de l'Institut d'Optique, CNRS and Université Paris-Sud, Campus Polytechnique, RD 128, F-91127 Palaiseau Cedex, France*

(Received 20 December 2007; published 5 May 2008)

We report fine-tuning of nonlinear interactions in a solid-state ring laser gyroscope by vibrating the gain medium along the cavity axis. We demonstrate both experimentally and theoretically that nonlinear interactions vanish for some values of the vibration parameters, leading to quasi-ideal rotation sensing. We eventually point out that our conclusions can be mapped onto other subfields of physics such as ring-shaped superfluid configurations, where nonlinear interactions could be tuned by using Feshbach resonance.

DOI: 10.1103/PhysRevLett.100.183901 PACS numbers: 42.65.Sf, 06.30.Gv, 42.55.Rz, 42.62.Eh

As pointed out in [1], most physical properties of lasers, superconductors, superfluid liquids and Bose-Einstein condensed gases come from the same phenomenon of macroscopic occupation of one or a few discrete quantum states. The possibility of exploiting those properties in ring-shaped configurations to create a new class of resonant rotation sensors, early suggested by [2,3], has been demonstrated experimentally on various physical systems [4–8]. All those macroscopic quantum devices share in common the fact that nonlinear interactions play a crucial role in their dynamics and can hinder or affect their ability to sense rotation, even when counteracted by other coupling sources [9]. Such interactions come, for example, [10] from the nonlinear properties of the laser gain medium in coherent photon optics and from elastic s-wave collisions in coherent atom optics.

The possibility of tuning or even suppressing nonlinear interactions in resonant macroscopic quantum rotation sensors hence appears as an important way of improving their characteristics. On that score, the experimental achievement of scattering length tuning by magnetically-induced Feshbach resonance in a Bose-Einstein condensate [11,12] opens new perspectives not only for coherent atom optics in general [13] but also more specifically for the field of rotation sensing with ring-shaped atom lasers, although in this latter case technical complexity has so far impeached the achievement of any interaction-free experiment.

Following the analogy between photon and atom optics [10], we present in this Letter a study of the control of nonlinear interactions in a solid-state ring laser. In this system, such interactions result mainly from mutual coupling between the counterpropagating modes induced by the population inversion grating established in the amplifying medium [14,15]. Their control is hence achieved by vibrating the gain crystal along the optical axis of the cavity. Using the quantitative information on the strength of the nonlinear interactions provided by the beat note between the counterpropagating laser beams [7], we demonstrate experimentally the possibility of suppressing these interactions for some discrete values of the amplitude of the crystal movement, leading to quasi-ideal rotation sensing on this device. In the limit of high vibration frequencies, we eventually show that the very simple rotation sensing condition derived for the solid-state ring laser can be mapped onto the equivalent condition for a toroidal Bose-Einstein condensed gas with scattering length tuning, issued from the combination of the toy model of [9] and of the simple description of Feshbach resonance presented in [11], which suggests that interaction control for the latter device could also improve its gyroscopic characteristics.

The solid-state ring laser gyroscope can be described semiclassically, assuming one single identical mode in each direction of propagation (something which is guaranteed by the attenuation of spatial hole burning effects thanks to the gain crystal movement [16]), one single identical state of polarization and plane wave approximation. The electrical field inside the cavity can then be written as follows:

$$E(x,t) = \mathrm{Re}\left\{\sum_{p=1}^{2} \tilde{E}_p(t) e^{i(\omega_c t + \mu_p k x)}\right\},$$

where $\mu_p = (-1)^p$ and where ω_c and k are, respectively, the angular and spatial average frequencies of the laser, whose longitudinal axe is associated with the x coordinate. In the absence of crystal vibration, the equations of evolution for the slowly varying amplitudes $\tilde{E}_{1,2}$ and for the population inversion density N have the following expression [7,15]:

$$\frac{d\tilde{E}_{1,2}}{dt} = -\frac{\gamma_{1,2}}{2}\tilde{E}_{1,2} + i\frac{\tilde{m}_{1,2}}{2}\tilde{E}_{2,1} + i\mu_{1,2}\frac{\Omega}{2}\tilde{E}_{1,2} + \frac{\sigma}{2T} \times \left(\tilde{E}_{1,2}\int_0^L N dx + \tilde{E}_{2,1}\int_0^L N e^{-2i\mu_{1,2}kx} dx\right),$$

$$\frac{\partial N}{\partial t} = W_{\rm th}(1+\eta) - \frac{N}{T_1} - \frac{aNE(x,t)^2}{T_1},$$

where $\gamma_{1,2}$ are the intensity losses per time unit for each mode, $\tilde{m}_{1,2}$ are the backscattering coefficients, Ω is the difference between the eigenfrequencies of the counterpropagating modes (including the effect of rotation, see further), σ is the laser cross section, T is the cavity round-trip time, η is the relative excess of pumping power above the threshold value $W_{\rm th}$, T_1 is the lifetime of the population inversion and a is the saturation parameter. Throughout this Letter we shall neglect dispersion effects, considering the fact that the Nd-YAG gain width is much larger than the laser cavity free spectral range. The backscattering coefficients, which depend on spatial inhomogeneities of the propagation medium [17], have the following expression [18]:

$$\tilde{m}_{1,2} = -\frac{\omega_c}{\bar{\varepsilon}cT}\oint_0^L \left[\varepsilon(x) - \frac{i\kappa(x)}{\omega_c}\right] e^{-2i\mu_{1,2}kx} dx, \qquad (1)$$

where $\varepsilon(x)$ and $\kappa(x)$ are, respectively, the dielectric constant and the fictitious conductivity along the cavity perimeter in the framework of an Ohmic losses model [19], where c is the speed of light in vacuum and where $\bar{\varepsilon}$ stands for the spatial average of ε. In order to counteract mode competition effects and ensure beat regime operation under rotation, an additional stabilizing coupling as described in [7] is introduced, resulting in losses of the following form:

$$\gamma_{1,2} = \gamma - \mu_{1,2}Ka(|\tilde{E}_1|^2 - |\tilde{E}_2|^2), \qquad (2)$$

where $\gamma = \bar{\kappa}/\bar{\varepsilon}$ is the average loss coefficient and where $K > 0$ represents the strength of the stabilizing coupling.

We assume the following sinusoidal law to account for the gain crystal vibration:

$$x_c(t) = \frac{x_m}{2}\sin(2\pi f_m t), \qquad (3)$$

where $x_c(t)$ is the coordinate, in the frame of the laser cavity, of a given reference point attached to the crystal, and where x_m and f_m are, respectively, the amplitude and the frequency of the vibration movement. The population inversion density function in the frame of the vibrating crystal $N_c(x,t)$ is ruled by the following equation:

$$\frac{\partial N_c}{\partial t} = W_{\rm th}(1+\eta) - \frac{N_c}{T_1} - \frac{aN_cE(x+x_c(t),t)^2}{T_1}, \qquad (4)$$

where $E(x,t)$ refers to the electric field in the cavity (non-vibrating) frame. Moreover, $N_c(x,t)$ can be deduced from its equivalent in the cavity frame $N(x,t)$ by the identity $N_c(x,t) = N(x+x_c(t),t)$, resulting in the following expressions:

$$\int_0^L N(x,t)dx = \int_0^L N_c(x,t)dx,$$

$$\int_0^L N(x,t)e^{2ikx}dx = e^{2ikx_c(t)}\int_0^L N_c(x,t)e^{2ikx}dx.$$

The backscattering coefficients (1) acquire in the presence of the crystal vibration the following time-dependent form:

$$\tilde{m}_{1,2}(t) = \tilde{m}^c_{1,2}e^{-2i\mu_{1,2}kx_c(t)} + \tilde{m}^m_{1,2}, \qquad (5)$$

where $\tilde{m}^c_{1,2}$ and $\tilde{m}^m_{1,2}$, which are time independent, account for the backscattering due, respectively, to the crystal at rest and to any other diffusion source inside the laser cavity (including the mirrors). As regards the difference Ω between the eigenfrequencies of the counterpropagating modes, it is due to the combined effects of the rotation (Sagnac effect [20]) and of the crystal movement in the cavity frame (Fresnel-Fizeau drag effect [21]), resulting in the following expression:

$$\frac{\Omega}{2\pi} = \frac{4A}{\lambda L}\dot{\theta} - \frac{2\dot{x}_c(t)l(n^2-1)}{\lambda L}, \qquad (6)$$

where A is the area enclosed by the ring cavity, $\lambda = 2\pi c/\omega_c$ is the emission wavelength, $\dot{\theta}$ is the angular velocity of the cavity around its axis, and l and n are, respectively, the length and the refractive index of the crystal (dispersion terms are shown to be negligible in this case).

The dynamics of the solid-state ring laser gyroscope with a vibrating gain medium is eventually ruled, in the framework of our theoretical description, by the following equations:

$$\begin{aligned}\frac{d\tilde{E}_{1,2}}{dt} = &-\frac{\gamma_{1,2}}{2}\tilde{E}_{1,2} + i\frac{\tilde{m}_{1,2}}{2}\tilde{E}_{2,1} + i\mu_{1,2}\frac{\Omega}{2}\tilde{E}_{1,2}\\ &+\frac{\sigma}{2T}\bigg(\tilde{E}_{1,2}\int_0^L N_c dx\\ &+\tilde{E}_{2,1}e^{-2i\mu_{1,2}kx_c}\int_0^L N_c e^{-2i\mu_{1,2}kx}dx\bigg),\end{aligned} \qquad (7)$$

where $\gamma_{1,2}$, x_c, N_c, $\tilde{m}_{1,2}$ and Ω obey, respectively, Eqs. (2)–(6). It comes out from this analysis that the solid-state ring laser benefits, as a rotation sensor, from the crystal vibration in three separate and complementary ways: (i) the contrast of the population inversion grating, which is responsible for nonlinear coupling, is reduced on both conditions that the amplitude of the movement is of the same order of magnitude than the step of the optical grating (typically a fraction of μm) and that the period of the movement $1/f_m$ is significantly larger than the population inversion response time T_1; the atomic dipoles are then no longer confined into a nodal or an antinodal area—see Eq. (4)—, and become sensitive to the time-average value of the electric field, which can be independent of their position on the crystal (at least when the laser is not rotating) provided the condition $J_0(kx_m) = 0$ is obeyed [22], J_0 referring to the zero-order Bessel's function; (ii) the light backscattered on the gain crystal from one mode into the other can be shifted out of resonance by the Doppler effect resulting from the crystal movement in the cavity frame; this phenomenon, which induces a decrease of the corresponding coupling strength, has previously

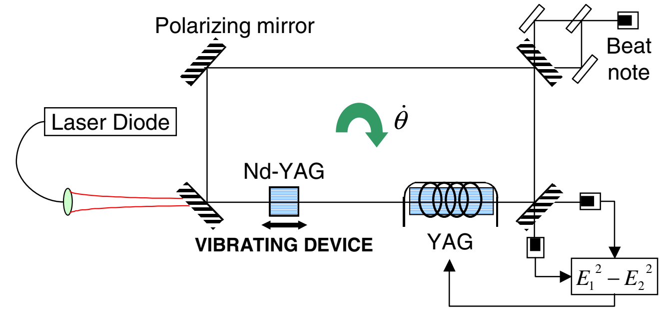

FIG. 1 (color online). Scheme of our experimental setup. The diode-pumped vibrating Nd-YAG crystal is placed inside a 22-cm ring cavity on a turntable. Losses of the form (2) are created by a feedback loop acting on a Faraday rotator (an additional YAG crystal inside a solenoid), in combination with a polarizing mirror and a slight nonplanarity of the cavity (not drawn here). Two photodiodes are used for generating the error signal of the feedback loop. A third photodiode measures the frequency of the beat note between the counterpropagating modes.

been reported in the case of vibrating mirrors [23,24]; in our model, it arises from the time-dependent phase factors $\exp(\pm 2ikx_c)$ in front of the coupling coefficients $\tilde{m}^c_{1,2}$ and $\int N_c dx$ in Eqs. (5) and (7); (iii) the frequency nonreciprocity between the counterpropagating modes due to the Fresnel-Fizeau dragging effect—Eq. (6)—has a similar role as the mechanical dithering typically used for circumventing the lock-in problem in the case of usual gas ring laser gyroscopes [25].

The solid-state ring laser setup we used in our experiment is sketched on Fig. 1. Thanks to the additional stabilizing coupling (2), a beat note signal is observed above a critical rotation speed, whose frequency is plotted on Fig. 2. It can be seen on this figure that the difference between the ideal Sagnac line and the experimental beat frequency, which is a direct measurement of the nonlinear interactions [7], is considerably reduced in the zone ranging from 10 to 40 deg/s. Some nonlinearities are observed around the discrete values $\dot{\theta} \simeq 55$ deg/s and $\dot{\theta} \simeq 165$ deg/s, in agreement with our theoretical model. As a matter of fact, analytical calculations starting from Eq. (7) reveal the existence of disrupted zones centered on discrete values of the rotation speed $\dot{\theta}_q$ obeying the following equation:

$$\frac{4A}{\lambda L}\dot{\theta}_q = q f_m \quad \text{where } q \text{ is an integer,} \tag{8}$$

the size of each disrupted zone being proportional to $J_q(kx_m)$. With our experimental parameters, the first critical velocity corresponds to $\dot{\theta}_1 = 55.5$ deg/s, the zones observed on Fig. 2 corresponding to the cases $q = 1$ and $q = 3$. The numerical simulations shown on the insert of this figure are in good agreement with our analytical and experimental data. Such a phenomenon of disrupted zones

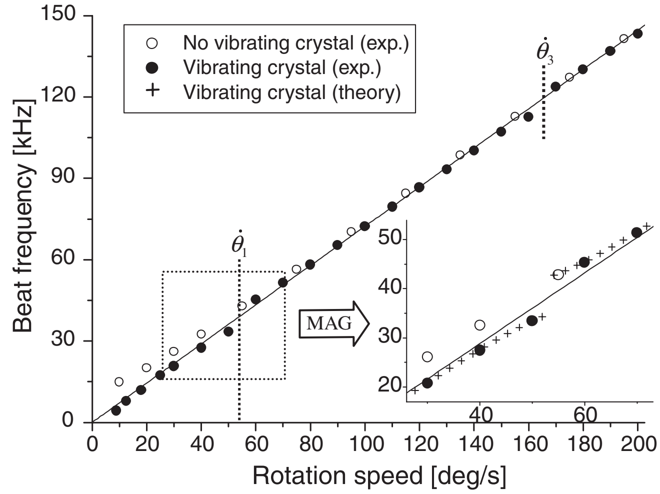

FIG. 2. Experimental beat frequency as a function of the rotation speed. White and black circles refer, respectively, to the situations where the crystal is at rest and where the crystal is vibrating with a frequency $f_m \simeq 40$ kHz and an amplitude $x_m \simeq 0.74$ μm. The inset shows a magnification around $\dot{\theta}_1$—see Eq. (8)—, together with theoretical predictions resulting from numerical simulations with the following measured [18] parameters: $\gamma = 15.34 \times 10^6$ s^{-1}, $\eta = 0.21$, $|\tilde{m}^c_{1,2}| = 1.5 \times 10^4$ s^{-1}, $|\tilde{m}^m_{1,2}| = 8.5 \times 10^4$ s^{-1}, $\arg(\tilde{m}^c_1/\tilde{m}^c_2) = \arg(\tilde{m}^m_1/\tilde{m}^m_2) = \pi/17$, $K = 10^7$ s^{-1}. Integration step is 0.1 μs, average values are computed between 8 and 10 ms.

has been reported previously in the case of gas ring laser gyroscopes with mechanical dithering [25].

The dependence of the beat frequency on the amplitude of the crystal movement is shown on Fig. 3, for a fixed rotation speed (200 deg/s). This graph illustrates the good agreement between our numerical simulations and our experimental data. Moreover, this is an experimental demonstration of the direct control of the strength of nonlinear interactions in the solid-state ring laser. In particular, for

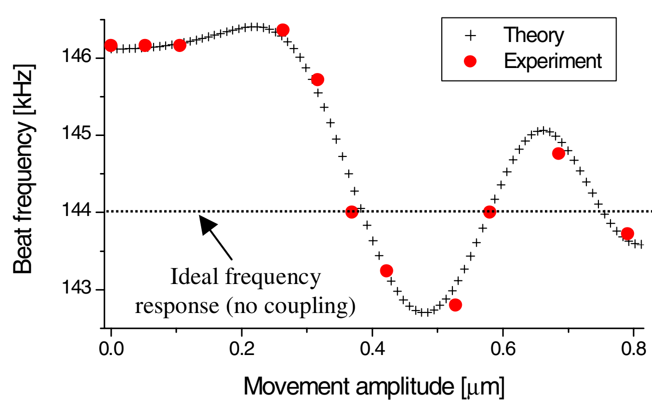

FIG. 3 (color online). Beat frequency as a function of the amplitude of the crystal movement for $\dot{\theta} = 200$ deg/s. The theoretical values (crosses) come from the numerical integration of Eq. (7) with the same parameters as Fig. 2.

some special amplitudes of the crystal movement, the influence of mode coupling vanishes, resulting in a beat frequency equal to the ideal Sagnac value.

This study suggests the use of a higher vibration frequency of the crystal, in order to increase the value of $\dot{\theta}_1$ as much as possible. When $f_m \gg |\Omega|/(2\pi)$, the strength of the nonlinear interactions is shown to be directly proportional to $J_0(kx_m)^2$, and the condition for rotation sensing reads

$$2K\eta > \tilde{N} J_0(kx_m)^2, \tag{9}$$

where $\tilde{N} = \gamma\eta/(1 + \Omega^2 T_1^2)$ is the strength of nonlinear interactions [7], and $J_0(kx_m)^2$ is the attenuation factor due to the crystal vibration. The similar condition for rotation sensing in the case of a toroidal Bose-Einstein condensate, as derived in [9], is $V_0 > g$ [where V_0 is the asymmetry energy and g the mean (repulsive) interaction energy per particle in the s-wave state]. It becomes, in the presence of Feshbach resonance induced by a magnetic field B as described in [11]:

$$V_0 > g\left(1 - \frac{\Delta}{B - B_0}\right), \tag{10}$$

where Δ and B_0 are characteristic parameters. In this equation, g represents the nonlinear interactions, and the attenuation factor is $1 - \Delta/(B - B_0)$. Condition (10) shows strong similarities with condition (9). In both cases, rotation sensing is favored if nonlinear interactions are lowered, the ideal case being $1 - \Delta/(B - B_0) = 0$ for the toroidal Bose-Einstein condensed gas and $J_0(kx_m) = 0$ for the solid-state ring laser. The parameter for the control of nonlinear interactions is the magnetic field B in the first case and the movement amplitude x_m in the second case.

In conclusion, we have developed a concrete method for tuning and suppressing nonlinear interactions in the case of a solid-state ring laser, by vibrating the gain crystal along the cavity axis. The value of the beat note frequency provides a direct measurement of the strength of nonlinear interactions, allowing the experimental proof of their fine-tuning. Our theoretical model shows a very good agreement with the experiment. This work demonstrates that interactions control in a resonant macroscopic quantum device can lead to quasi-ideal rotation sensing in the case of a solid-state ring laser. Furthermore, following the analogy between photon and atom optics, we have pointed out that the rotation sensing condition for our experimental device can be mapped onto other systems like ring-shaped Bose-Einstein condensed gas with magnetically induced Feshbach resonance. This suggests that scattering length control of ultracold quantum gases in toroidal traps could dramatically improve their gyroscopic capacity, which could open the way to a new generation of atomic rotation sensors.

The authors thank M. Defour, M. Mary, E. Bonnaudet, and Thales Aerospace Division for constant support. They are also grateful to A. Aspect and A. Mignot for fruitful discussions, and to F. Grabisch for his contribution to the numerical simulations.

*sylvain.schwartz@thalesgroup.com

[1] J. Bardeen, Phys. Today **43**, No. 12, 25 (1990).
[2] A. H. Rosenthal, J. Opt. Soc. Am. **52**, 1143 (1962).
[3] F. Bloch, Phys. Rev. A **7**, 2187 (1973).
[4] W. Macek and D. Davis, Appl. Phys. Lett. **2**, 67 (1963).
[5] S. Vitale *et al.*, Phys. Rev. B **39**, 11 993 (1989).
[6] O. Avenel, P. Hakonen, and E. Varoquaux, Phys. Rev. Lett. **78**, 3602 (1997).
[7] S. Schwartz *et al.*, Phys. Rev. Lett. **97**, 093902 (2006).
[8] C. Ryu *et al.*, Phys. Rev. Lett. **99**, 260401 (2007).
[9] A. Leggett, Rev. Mod. Phys. **73**, 307 (2001).
[10] S. L. Rolston and W. D. Phillips, Nature (London) **416**, 219 (2002).
[11] S. Inouye *et al.*, Nature (London) **392**, 151 (1998).
[12] Ph. Courteille *et al.*, Phys. Rev. Lett. **81**, 69 (1998).
[13] M. Fattori *et al.*, Phys. Rev. Lett. **100**, 080405 (2008)
[14] P. A. Khandokhin and Y. I. Khanin, J. Opt. Soc. Am. B **2**, 226 (1985).
[15] N. Kravtsov, E. Lariontsev, and A. Shelaev, Laser Phys. **3**, 21 (1993).
[16] H. Danielmeyer and W. Nilsen, Appl. Phys. Lett. **16**, 124 (1970).
[17] R. Spreeuw *et al.*, Phys. Rev. A **42**, 4315 (1990).
[18] S. Schwartz *et al.*, Phys. Rev. A **76**, 023807 (2007).
[19] A. Siegman, *Lasers* (University Science Books, Mill Valley, California, 1986).
[20] G. Sagnac, C R Acad. Sci. **157**, 708 (1913).
[21] H. R. Bilger and W. K. Stowell, Phys. Rev. A **16**, 313 (1977).
[22] H. Sabert and R. Ulrich, Appl. Phys. Lett. **58**, 2323 (1991).
[23] R. A. Patterson *et al.*, Proc. SPIE Int. Soc. Opt. Eng. **487**, 78 (1984).
[24] M. Lai *et al.*, Opt. Lett. **17**, 1535 (1992).
[25] W. Chow *et al.*, Rev. Mod. Phys. **57**, 61 (1985).